

MUSK, a new target for mutations causing congenital myasthenic syndrome

Frédéric Chevessier¹, Brice Faraut¹, Aymeric Ravel-Chapuis², Pascale Richard^{1,3}, Karen Gaudon^{1,3}, Stéphanie Bauché¹, Cassandra Prioleau¹, Ruth Herbst⁶, Evelyne Goillot², Christine Ios¹, Jean-Philippe Azulay⁷, Shahram Attarian⁷, Jean-Paul Leroy^{1,8}, Emmanuel Fournier⁴, Claire Legay⁹, Laurent Schaeffer², Jeanine Koenig^{1,10}, Michel Fardeau¹, Bruno Eymard^{1,5}, Jean Pouget⁷ and Daniel Hantai^{1,*}

¹INSERM U582 & IFR 'Cœur, Muscle, Vaisseaux', Institut de Myologie, Hôpital de la Salpêtrière and Université Pierre et Marie Curie, Paris, France, ²CNRS/ENS UMR 5161 & IFR128, École Normale Supérieure, Lyon, France, ³Unité Fonctionnelle de Cardiogénétique et Myogénétique, Service de Biochimie B & IFR 'Cœur, Muscle, Vaisseaux,' and ⁴Service d'Electrophysiologie & IFR 'Neurosciences' and ⁵Fédération de Neurologie Mazarin & IFR 'Neurosciences', Hôpital de la Salpêtrière, Paris, France, ⁶Brain Research Institute, Medical University Vienna, Vienna, Austria, ⁷Service de Neurologie et Maladies Neuromusculaires, Hôpital Universitaire La Timone & IFR CNRS 'Sciences du Cerveau et de la Cognition', Marseilles, France, ⁸CHU Morvan, Brest, France, ⁹CNRS UMR 8544, École Normale Supérieure, Paris, France and ¹⁰Université Bordeaux II, Bordeaux, France

Received September 16, 2004; Revised and Accepted October 12, 2004

We report the first case of a human neuromuscular transmission dysfunction due to mutations in the gene encoding the muscle-specific receptor tyrosine kinase (MuSK). Gene analysis identified two heteroallelic mutations, a frameshift mutation (c.220insC) and a missense mutation (V790M). The muscle biopsy showed dramatic pre- and postsynaptic structural abnormalities of the neuromuscular junction and severe decrease in acetylcholine receptor (AChR) ϵ -subunit and MuSK expression. *In vitro* and *in vivo* expression experiments were performed using mutant MuSK reproducing the human mutations. The frameshift mutation led to the absence of MuSK expression. The missense mutation did not affect MuSK catalytic kinase activity but diminished expression and stability of MuSK leading to decreased agrin-dependent AChR aggregation, a critical step in the formation of the neuromuscular junction. In electroporated mouse muscle, overexpression of the missense mutation induced, within a week, a phenotype similar to the patient muscle biopsy: a severe decrease in synaptic AChR and an aberrant axonal outgrowth. These results strongly suggest that the missense mutation, in the presence of a null mutation on the other allele, is responsible for the dramatic synaptic changes observed in the patient.

INTRODUCTION

Congenital myasthenic syndromes (CMS) are rare hereditary diseases characterized by dysfunction of neuromuscular transmission resulting in fatigable muscle weakness. CMS form a heterogeneous group of disorders which are classified as originating from presynaptic, synaptic or postsynaptic defects (1,2). Within the class of postsynaptic CMS, mutations in genes coding for the different AChR subunits have been identified as causing either kinetic abnormalities of AChR activity

or low AChR levels at the neuromuscular junction (NMJ) (1). Reduced AChR content has been shown to originate also from mutations within the rapsyn gene (3,4).

During NMJ development, the agrin–MuSK–rapsyn pathway plays a key role in the organization of the postsynaptic scaffold (5–7). MuSK is a muscle-specific receptor tyrosine kinase critical for synaptic differentiation since MuSK-deficient mice die at birth from respiratory failure caused by aberrant innervation and lack of postsynaptic differentiation (7). The best studied mechanism of the NMJ

*To whom correspondence should be addressed at: INSERM U582, Institut de Myologie, Hôpital de la Salpêtrière, 47, Boulevard de l'Hôpital, 75651 Paris, Cedex 13, France. Tel: +33 142165706; Fax: +33 142165700; Email: d.hantai@myologie.chups.jussieu.fr

differentiation program is AChR clustering beneath the nerve terminal. First, the nerve releases a heparan sulfate proteoglycan called agrin, which activates MuSK. MuSK activation leads to the phosphorylation of the AChR β -subunit and triggers AChR aggregation via the cytoplasmic effector protein rapsyn (8–12). Thereafter, AChR synthesis at the NMJ results from the compartmentalization of its transcription to subsynaptic nuclei. This is especially the case for the adult ϵ -subunit AChR, which replaces the embryonic γ -subunit AChR, within the AChR pentamer (9). MuSK also induces the aggregation of receptor tyrosine kinases of the ErbB family in the postsynaptic membrane, which are activated by neuregulin-1, a disputed factor for AChR transcription (13,14). MuSK signaling is also required for presynaptic differentiation (7). The aberrant innervation observed in MuSK-null mutant mice could result from the absence of unknown MuSK-dependent retrograde signaling components that are normally expressed by synaptic nuclei (7,15).

MuSK is encoded by the gene *MUSK* located on chromosome 9 in q31.3q32. Its mRNA consists of 2666 bp (NM005592) and comprises 14 exons coding for a protein of 869 amino acids (NP005583, December 2003). Like all tyrosine kinase receptors, this protein includes a large ectodomain containing IgG-like motifs, a transmembrane region and a cytoplasmic domain that characterizes a functional tyrosine kinase located in humans between residues Q569 and V859. Human and rat MuSK are highly homologous especially in their intracellular domains which reach 97% identity (16). Three DNA polymorphisms have recently been reported in a patient suffering from MuSK-seropositive autoimmune myasthenia gravis (17).

In this article, we report a case of a CMS patient carrying two heterozygous mutations in *MUSK*. MuSK constructs reproducing these two mutations were generated and transfected both in cell culture systems and *in vivo* in mouse muscle by electroporation. This allowed the evaluation of the pathogenic consequences of these human mutations.

RESULTS

Study of the patient

Clinical data. The patient is a 27-year-old woman born to non-consanguineous parents. Clinical symptoms of ptosis and respiratory distress appeared in the neonatal period. She needed tracheostomy at the age of 45 days and had two respiratory distress episodes at the ages of 6 and 8 months. At the age of 6 years, she had surgical treatment for left ptosis. The course of the disease during childhood and adolescence was favorable. Clinical symptoms improved, and the patient had no further severe respiratory episodes. The patient only complained of slight eyelid ptosis, fatigability on walking and the inability to have sport activities. Symptoms fluctuated. At the age of 22, 3 months into her first pregnancy, the patient suffered from aggravating symptoms of generalized weakness of the superior and inferior limb muscles with falls. She had masticatory difficulties, swallowing disturbances and nasal voice. The diagnosis of myasthenic syndrome was made. Tests for the presence of AChR and MuSK antibodies in serum were negative. Clinical electrophysiology studies

showed decremental responses on 3 Hz stimulation of trapezius (–56%) and eyelid orbicular muscles (–17%). The patient was treated with acetylcholinesterase inhibitors (pyridostigmine up to 720 mg per day) without any real efficacy. Subsequently, 3,4-diaminopyridine was added at 50 mg per day and a clear improvement of clinical symptoms was observed. At the present time, the woman presents bilateral ptosis, an upward gaze limitation, a weakness of neck extensor muscles, and a predominantly proximal weakness of the superior limbs. Symptoms fluctuate with episodes of fatigability. Respiratory distress and bulbar disorders are absent. She is treated with pyridostigmine at 120–240 mg per day and 3,4-diaminopyridine at 30–50 mg per day.

The disease inheritance is autosomal recessive. On the basis of patient's statement, both her mother and her deceased father were not affected by any neuromuscular disorder. One brother of the patient who would have been 24 years of age today also suffered from CMS. He presented with neonatal hypotonia, respiratory failure, vocal cord paralysis and needed tracheostomy. A muscle biopsy was done and microscope sections were done before he died at 1.5 years of age. This allowed us to extract his DNA from the sections for genetic analysis. Another brother aged 29 presents with a genetic abnormality (fragile-X syndrome) but without any clinical or electromyographic sign of neuromuscular dysfunction.

Immunocytochemical analysis of patient muscle biopsy. Whole mount preparations, stained with both AChR and neurofilament, showed that in a control biopsy the nerve terminal appeared normal in a fork-shape and innervated a well defined synaptic structure. Conversely, in the patient the nerve terminal sprouted and sent extensions, which contacted several small synaptic cups that were separated from each other (Fig. 1A). In other preparations, the nerve terminals ended with large growth cones that did not contact AChR clusters (data not shown).

Double labeling of AChR and MuSK on cryostat sections showed that in the control patient AChR was present as a well defined patch on the surface of the fiber and colocalized with MuSK (Fig. 1B). In the patient, several AChR patches were often observed at the surface of single muscle fibers. AChR staining was less intense as measured on at least 12 control and patient NMJs ($45 \pm 4\%$ of controls). MuSK staining was also markedly reduced at the NMJ ($52 \pm 6\%$ of controls) and spread away from the NMJ to the extra-synaptic zone (Fig. 1B). Such MuSK delocalization was not observed in biopsies from CMS patients with mutations in genes other than *MUSK* (data not shown).

Mutation analysis and polymorphism identification. The two major genes (*CHRNE* and *RAPSN*) involved in postsynaptic CMS were initially sequenced and no mutations were found. As the morphological studies indicated perturbations in MuSK levels and localization, the 14 exons and their flanking regions were sequenced. We identified two heteroallelic mutations in the index patient (Fig. 2A). The first mutation is an insertion of one C nucleotide in exon 3 at position 220 (c.220insC) of the coding sequence. This insertion is predicted to disrupt the reading frame at codon 73–74 and to introduce a

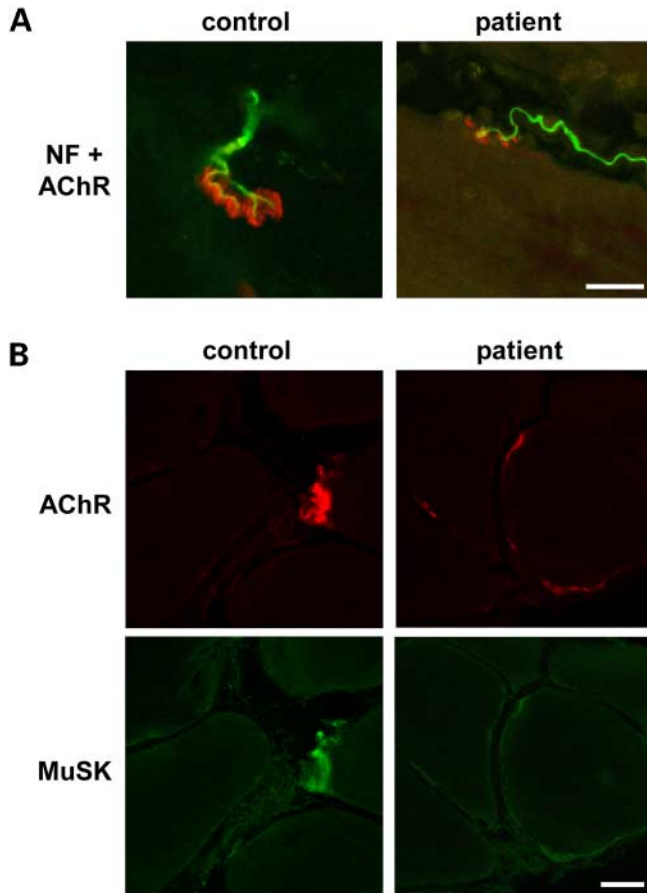


Figure 1. Axonal endings sprout and MuSK is delocalized from the NMJ in this patient muscle biopsy. (A) Whole mount preparations were stained for AChR with TRITC- α -BGT in red and for axon terminals with FITC-200 kDa neurofilament (NF) antibody in green. Note that the axonal branch sends sprouts from one small separated NMJ cup to another in the patient, whereas it classically ends as a fork and innervates a well-defined synaptic structure in the control. Calibration bar = 20 μ m and applies to both prints. (B) Cryostat sections were double labeled for AChR in red and for MuSK in green. Note that in the patient MuSK and AChR are attenuated. MuSK is not strictly localized at the NMJ but spreads away from the NMJ around the muscle fiber. Calibration bar = 20 μ m and applies to the four prints.

premature termination codon in exon 3 (codon 92). The second mutation is a G \rightarrow A transition at nucleotide 2368 of the coding sequence in exon 14 (c.2368G \rightarrow A) leading to the missense V790M mutation. This mutation is located in the C-terminus domain of the protein corresponding to the conserved catalytic tyrosine kinase domain (16) and the mutated valine is highly conserved between species (18). In order to confirm the pathogenic role of the two variants found, we determined the genetic status of the deceased affected brother of the proband from whom biopsy sections done 24 years ago were available. We found that the affected brother was also a carrier of the same two mutations. Genetic analysis in available relatives revealed, according to the recessive mode of inheritance in this family, that the insertion was transmitted by the individual I-I (deceased father with no DNA available) to individuals II-1 and II-3 and the missense V790M mutation was transmitted by individual I-2 (mother) to affected individuals II-1 and II-3 and unaffected individual

II-2 (Fig. 2B). Extensive screening for *MUSK* revealed frequently found variants which were thus considered as polymorphisms. These are IVS2 + 28: a \rightarrow t, IVS3 - 20: t \rightarrow c in intronic flanking sequences and two silent polymorphisms at residues E134 (GAG-GAA) and N179 (AAC-AAT). E134 and N179 had a percentage heterozygosity of 30 and 27%, respectively.

Gene expression analysis of patient muscle biopsy. Since extra-synaptic staining of α -bungarotoxin (α -BGT) was detectable on biopsy sections, we sought to determine whether the presence of extra-synaptic AChR could be due to a compensatory upregulation of the embryonic AChR γ -subunit, which is normally not expressed in adult muscle. The level of AChR γ -subunit expression versus that of adult AChR ϵ -subunit expression was measured by quantitative real-time PCR (QRT-PCR). The results were normalized to β -actin for the AChR γ -subunit. Because the AChR ϵ -subunit is only expressed at the NMJ, the results from various biopsy sections had to be normalized to the average number of NMJs per section or to the expression of a synapse-specific gene not affected by the myasthenic syndrome. Considering that presynaptic terminal Schwann cells were present in the patient and gene expression in these cells was less affected than in postsynaptic nuclei, ErbB3, a Schwann cell-specific gene, was chosen as such (19). As shown in Figure 3, the synaptic levels of AChR ϵ -subunit mRNA were decreased in the patient biopsies compared with control biopsies leading to a low level of synaptic AChR as shown by immunocytochemistry. Conversely, the overall levels of AChR γ -subunit mRNA were increased in the patient biopsies compared with control biopsies.

The expression of AChR γ -subunit may be due to a compensation for changes in the AChR ϵ -subunit expression or it could alternatively be a direct consequence of changes in muscle electrical activity (13). Therefore, the expression of the myogenin gene, which is strictly regulated by muscle electrical activity, was measured (20). The levels of myogenin mRNA normalized to β -actin were increased in the patient biopsies, compared, with control biopsies, thus suggesting that the expression of the AChR γ -subunit is a consequence of the perturbation of muscle electrical activity, resulting from altered synaptic transmission.

Functional evaluation of *MUSK* mutations

In order to investigate whether the mutations detected did indeed cause the myasthenic syndrome observed in the patient, site-directed mutagenesis of a rat *MuSK* cDNA was used to generate two *MuSK* constructs that reproduced the two mutations: c.220insC and c.2365G \rightarrow A (V789M) detected in the patient. Human and rat *MuSK* sequences are highly homologous but differ in their numbering scheme. This explains the numbering difference observed between the human (V790M) and the rat (V789M) corresponding mutation. For simplification, the symbol insC for the construct corresponding to the frameshift mutation and G \rightarrow A for that corresponding to the missense mutation will be used in all subsequent functional experiments.

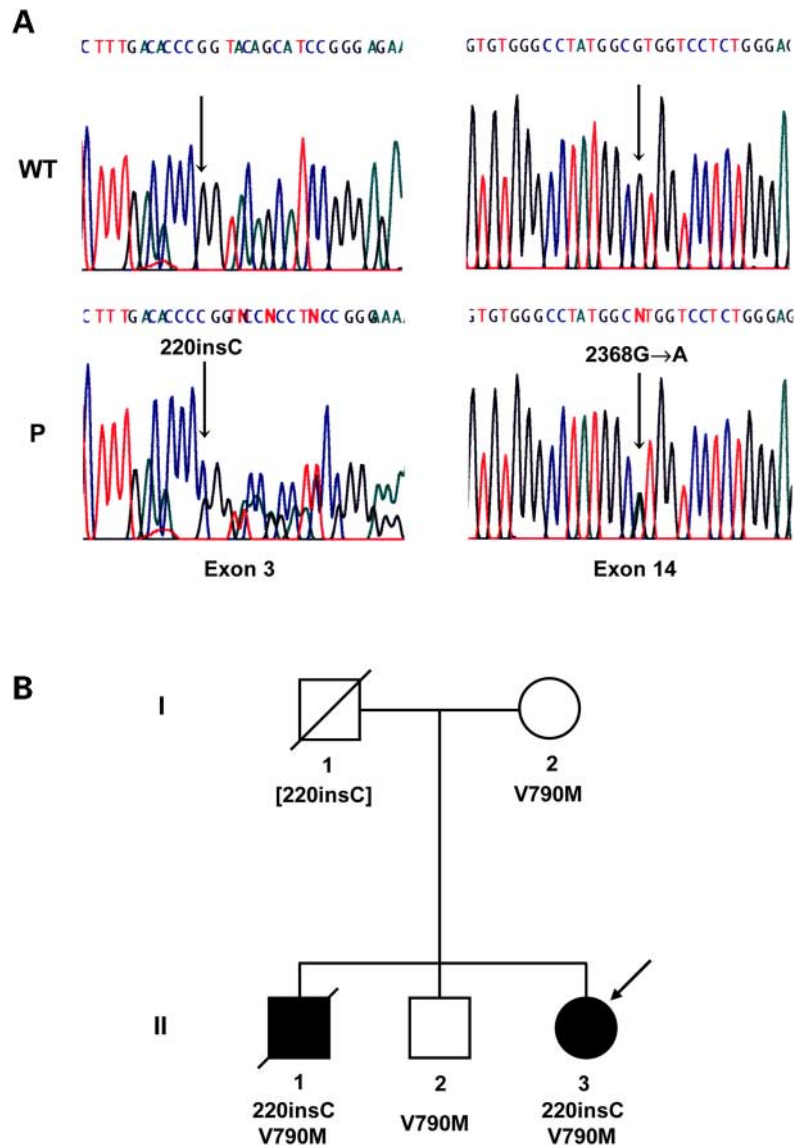


Figure 2. Identification of mutations in *MUSK* and hereditary transmission. (A) Sequence chromatograms from normal individual (wild-type, WT) and affected individual (proband, P) are shown together with the expected nucleotide change. Nucleotide variations are indicated by an arrow. In the proband, one allele bears the 220insC frameshifting mutation, the other bears the 2368G → A missense mutation which induces V790M in MuSK. (B) Pedigree of the family. The proband is indicated by an arrow. The two mutations transmitted in the family are indicated below the symbols.

MuSK mutant phenotypes in culture. Changes in the expression and stability of the MuSK mutant proteins: MuSK mutants and GFP construct were cotransfected in COS cells and western blots were performed on cell extracts with antibodies raised against GFP and the C-terminal part of MuSK (21). As shown in Figure 4A, in wild-type MuSK and G → A mutant transfected cells, a band corresponding to MuSK was detected. The amount of MuSK protein in the G → A mutant-expressing cells was reduced compared to the levels present in the wild-type MuSK-expressing cells. No band was detected with the cells expressing either the empty pcDNA3 vector or the insC mutant. No lower molecular weight band, which would have indicated the expression of a truncated protein, was detected by a N-terminal MuSK polyclonal antibody (data not shown). GFP was used to determine

the transfection efficiencies in all conditions. To investigate whether the diminution in MuSK expression due to the G → A mutation was the result of an instability of the mutant molecule in muscle cells, C2C12 cells were transiently transfected with hemagglutinin (HA)-tagged MuSK constructs. Transfection efficiencies were monitored by cotransfecting a GFP expression vector. The stability of wild-type and mutant MuSK was evaluated in the presence of the translation inhibitor cycloheximide (Fig. 4B). The difference between the mutant and wild-type MuSK protein levels was also observed here. In addition, the mutant MuSK was degraded much faster than the wild-type MuSK, thus demonstrating that the G → A mutation destabilizes MuSK protein.

The G → A mutated MuSK diminishes agrin-dependent AChR aggregation and MuSK phosphorylation: In these

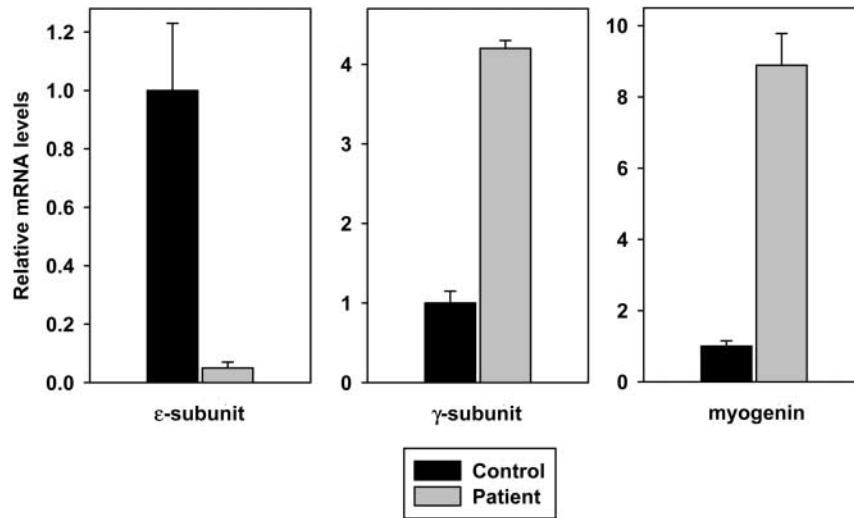


Figure 3. Quantitative measurements of AChR ϵ - and γ -subunit mRNA as well as myogenin mRNA in patient muscle biopsy. Gene expression was evaluated by quantitative RT-PCR on total RNA extracted from biopsies. AChR ϵ -subunit mRNA levels were normalized to ErbB3. AChR- γ and myogenin mRNA levels were normalized to β -actin. The expression levels of the genes tested are given as ratios of their expression levels in control biopsies. Error bars correspond to the standard deviation of at least 3 skeletal muscle biopsy samples from control individuals and from the patient.

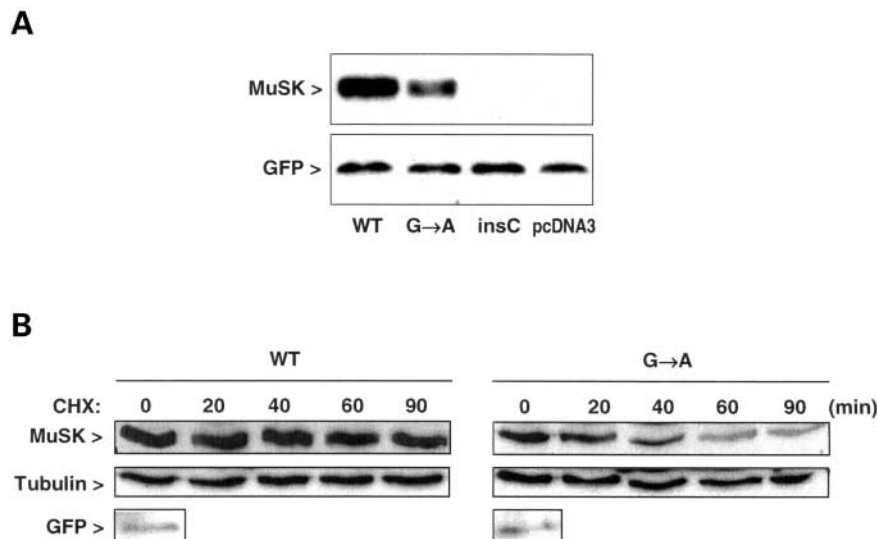


Figure 4. Cell expression and stability of MuSK mutants reproducing the human mutations (A) MuSK protein expression in extracts of COS cells after transfection with MuSK mutated and GFP constructs. Western blot with polyclonal MuSK and monoclonal GFP antibodies showed normal expression of the wild-type MuSK protein (WT), diminished expression of the G \rightarrow A mutant MuSK and no expression of the insC mutant or the pcDNA3 vector alone in transfected COS cells. GFP cotransfection was used to verify transfection efficiency. (B) Hemagglutinin (HA)-tagged MuSK and GFP constructs were transfected into C2C12 cells. Transfected C2C12 cells were treated with cycloheximide (CHX) and at different times after addition of CHX, amounts of WT and mutant MuSK were analyzed by western blot with anti-HA antibody. Alpha-tubulin was used as an internal control and transfection efficiency was verified with anti-GFP antibody. Mutant G \rightarrow A protein decreased significantly 40 min after CHX addition whereas no obvious decrease of the WT MuSK protein was observed at 90 min.

experiments, we used MuSK $-/-$ cell lines stably infected with a recombinant retrovirus expressing either wild-type or G \rightarrow A mutated MuSK (12). We used three G \rightarrow A clones expressing MuSK to the same level as the wild-type clone as verified by western blotting (Fig. 5A). As previously described (12, 22), agrin failed to induce AChR aggregation in MuSK $-/-$ myotubes. Wild-type MuSK expression restored agrin-induced AChR aggregation in these cells. Cells expressing G \rightarrow A MuSK mutant formed about half of the AChR clusters obtained in wild-type MuSK-expressing

cells (Fig. 5B). Using anti-phosphotyrosine immunoblotting we observed that, in the presence of agrin, G \rightarrow A MuSK was phosphorylated to a lesser extent than wild-type MuSK (Fig. 5B). As equivalent amounts of MuSK were present in the cells, this suggests that the G \rightarrow A mutation not only affects the stability of the protein as previously described but also alters the agrin-induced MuSK phosphorylation leading to AChR aggregation.

The G \rightarrow A mutant MuSK does not affect catalytic kinase activity: As the G \rightarrow A mutation is located in the kinase

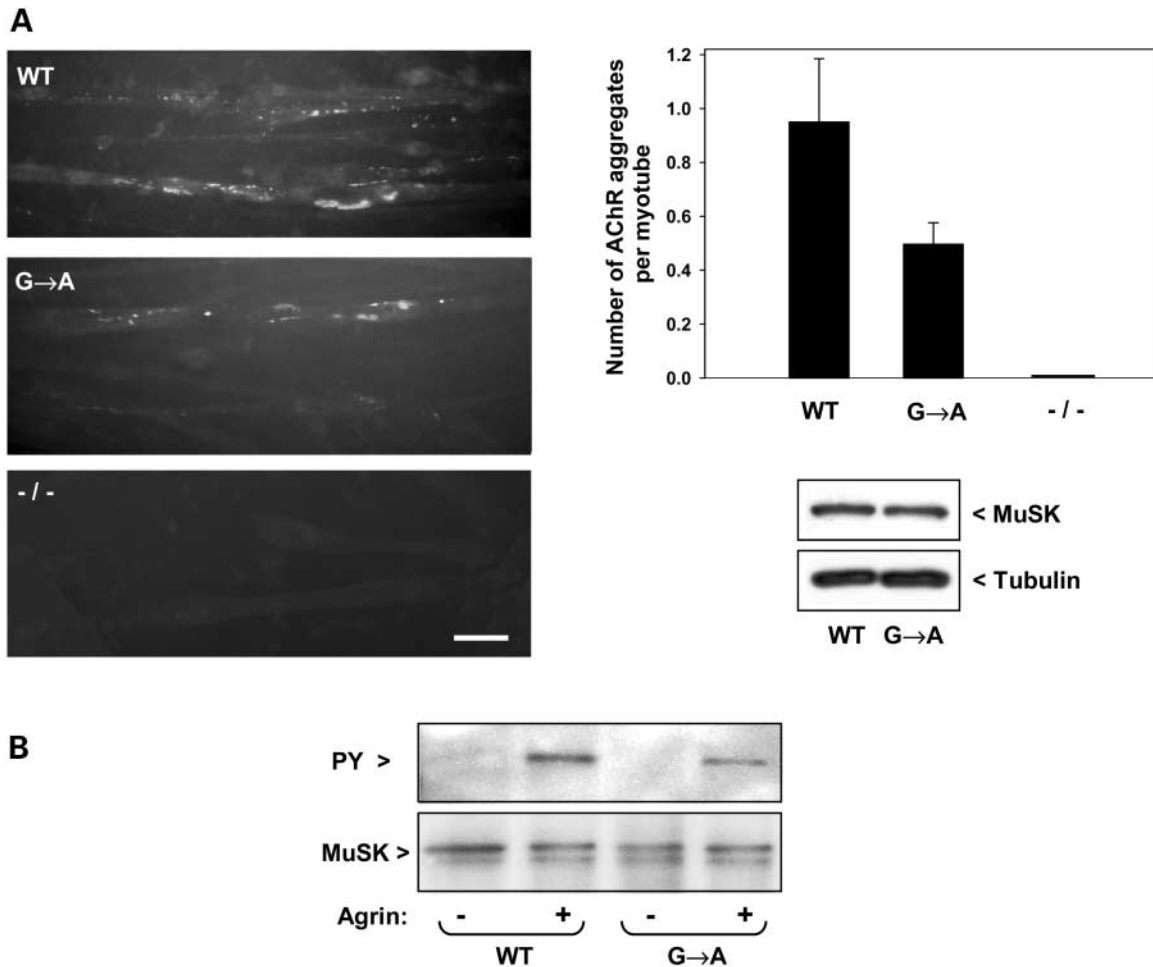


Figure 5. Effects of the G → A mutant MuSK on agrin-dependent AChR aggregation and MuSK phosphorylation. (A) WT MuSK rescued agrin-induced AChR aggregation in retrovirally infected stable cell lines. G → A rescued it too but to a lesser extent. No agrin-induced AChR clusters were detected in MuSK $-/-$ myotubes. Calibration bar = 50 μ m and applies to all prints. The graph represents the number of AChR aggregates per myotube which crossed the field from 3 independent experiments (15 fields in each Petri dish were randomly counted for each condition for each experiment). The blot shows that equal amounts of MuSK were expressed by cell lines expressing WT or G → A MuSK; alpha-tubulin was used to verify protein loads. (B) Agrin dependence of MuSK tyrosine phosphorylation in retrovirally infected stable cell lines expressing either WT or G → A MuSK to the same level. After immunoprecipitation, MuSK was visualized by phosphotyrosine immunoblotting (PY). The blot was stripped and reprobbed with MuSK antibodies (MuSK). This experiment shows a decrease of agrin-dependent MuSK phosphorylation.

domain, we measured ability of G → A mutant MuSK to phosphorylate itself and to transphosphorylate the substrate peptide EKY after ATP stimulation. For these experiments, equal amounts of wild-type and G → A mutant HA-tagged MuSK were immunoprecipitated from transfected COS cells and the immunoprecipitates were incubated in the presence of radiolabeled ATP. MuSK autophosphorylation was measured by phosphoimager analysis. The G → A mutation induced no significant change in MuSK autophosphorylation (Fig. 6A). Exogenous kinase activity of MuSK was measured by adding the EKY peptide to the same immunoprecipitates and also revealed no significant changes in the kinase activity of the G → A mutant as compared with the wild-type protein (Fig. 6B).

Effects of MuSK mutants in vivo. To address *in vivo* the consequences of the G → A mutation in *MuSK*, wild-type and

mutated *MuSK* expression vectors were electroporated in the mouse tibialis anterior muscle to evaluate their effect on AChR ϵ -subunit expression and on NMJ morphology. The mutant *MuSK* expression vectors were co-electroporated with a nuclear cyan fluorescent protein (CFP) expression vector (pECFPnuc) to allow microdissection of CFP-positive fibers for morphological NMJ analysis or RNA extraction and gene expression analysis by QRT-PCR. The contralateral muscle received either empty or wild-type *MuSK* expression vector, together with pECFPnuc.

The G → A mutation alters the structure of NMJs: Eight days after electroporation, the size and morphology of NMJs (Fig. 7A) of muscle fibers transfected with wild-type *MuSK*, pcDNA3 or with insC mutated *MuSK* remained roughly normal. Conversely, when transfected with the G → A *MuSK* expression vector, NMJ morphology was dramatically modified: NMJs were composed of small cups and short

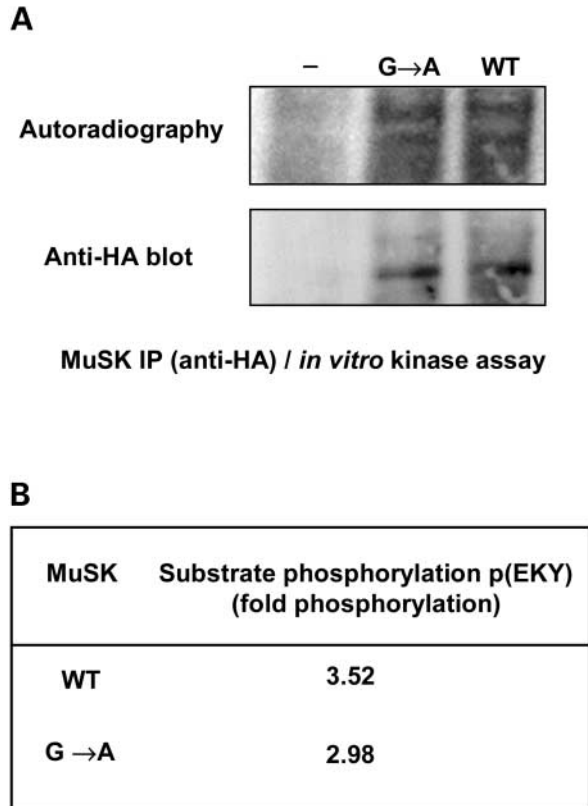


Figure 6. G → A MuSK autophosphorylation and kinase activity after ATP stimulation. (A) *In vitro* phosphorylation of HA-tagged wild-type (WT) and G → A MuSK after transfection of the corresponding constructs into COS cells. Anti-HA-11 and anti-HA-12CA5 monoclonal antibodies were used for immunoprecipitation and western blotting, respectively. Control (–) represents untransfected COS cells. Both WT and mutant MuSK were phosphorylated similarly *in vitro*. (B) *In vitro* kinase assay shows that the p(EKY) peptide is phosphorylated by both WT and G → A mutant forms of MuSK. No clear-cut changes in kinase activity are observed between the G → A mutant and WT MuSK.

gutters; the nerve terminals were abnormally branched and exhibited terminal and ultraterminal sprouting. The ratio of the nerve terminal and ultraterminal sprout over the synaptic gutter was quantitated in at least 15 NMJs for each condition and found to be increased more than two times in the presence of the G → A mutant in comparison with the other conditions (Fig. 7B). In addition, many nerve terminals with growth cones not associated with AChR aggregates were present. Furthermore, the nerve terminals of the wild-type *MuSK* electroporated NMJ were visualized strongly by an anti-200 kDa mature neurofilament (NF-H) antibody but faintly by an anti-160 kDa immature neurofilament (NF-M) antibody, whereas in the G → A electroporated mouse only the 160 kDa neurofilament antibody stained the terminal arborizations and its sprouting elements.

In vivo gene expression of the AChR ϵ -subunit is affected by mutated *MuSK* (Fig. 7C): The AChR ϵ -subunit gene is exclusively expressed by synaptic nuclei. Thus, when AChR ϵ -subunit expression was measured in microdissected fibers 3 days after electroporation, the results had to be normalized in some way to the number of NMJs harvested in each

microdissection. The AChR ϵ -subunit mRNA levels were normalized to the levels of ErbB3 mRNA, which essentially accumulates in terminal Schwann cells in the presynaptic compartment (19). As expected, when the wild-type *MuSK* expression vector was electroporated in skeletal muscle, the levels of AChR ϵ -subunit mRNA increased. Conversely, when the G → A *MuSK* mutant was expressed, the AChR ϵ -subunit expression remained slightly above the basal level observed with the empty or insC mutated *MuSK* vectors and clearly decreased in comparison with wild-type MuSK.

The dramatic modification of NMJ morphology and the lower induction of AChR ϵ -subunit mRNA expression suggest that the forced expression of G → A *MuSK* mutant induces a functional dysinnervation.

DISCUSSION

We report here the description of a case of CMS associated with heteroallelic mutations in the *MuSK* gene: a frameshift mutation (220insC) and a missense mutation (V790M). The frameshift mutation leads to an absence of the protein, whereas the missense mutation induces the expression of a functionally abnormal MuSK.

This CMS is of autosomal recessive inheritance. The patient's father who carries the frameshift mutation was not clinically affected due to the sole expression of his normal allele. The patient's mother who carries the missense mutation and a normal allele does not suffer from CMS, as the normal MuSK is likely to compensate for the pathogenic effect of G → A MuSK. In the patient like in her deceased brother, this pathogenic effect is not compensated because the other allele is a null allele. Both sibs had severe respiratory distress in the neonatal period but the outcome was fatal in the brother and favorable in the sister. With the same two mutations, the two sibs differ in their phenotypic expression and especially in the clinical course of the disease. These phenotypic variations are not specific and may be encountered in other types of CMS (2).

At the NMJ, MuSK is known to be involved in the regulation of AChR aggregation in the embryo (9) and AChR expression both during development (9) and in the adult (23). Evidence is presented that the missense mutation diminished AChR aggregation when expressed in muscle cells in culture and both AChR expression in the patient muscle biopsy and in transfected mouse muscle. In the latter, the forced expression of the missense mutation induced major synaptic changes similar to those observed in the patient muscle biopsy.

Consequences of the MuSK mutations for agrin-dependent AChR aggregation

As expected from the cDNA sequence, the insC mutation abolished the expression of MuSK. The G → A mutation caused a reduction in MuSK protein levels in transfected COS and C2C12 cells. With the latter cells, we have demonstrated using cycloheximide that the reduced levels of mutant MuSK were due to accelerated degradation. To determine whether this diminution of MuSK expression or other

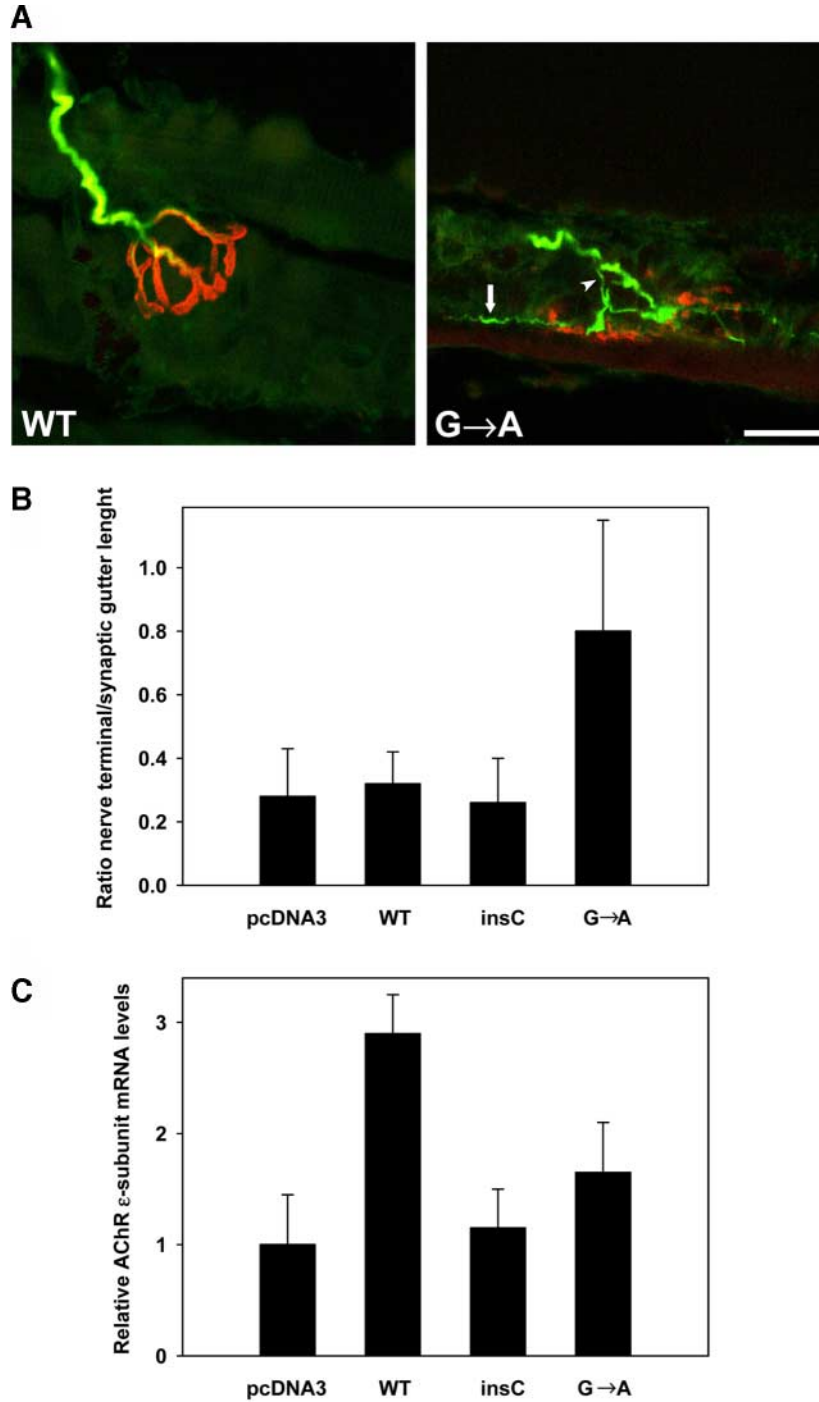


Figure 7. Effects of G → A MuSK recombinant electroporated in wild-type mouse skeletal muscle. (A) Terminal sprouting at NMJ was induced by G → A mutant *MuSK* 8 days after electroporation. In the wild-type (WT) *MuSK* electroporated mouse tibialis anterior muscle, the motor axon stained for 200 kDa neurofilament (in green) terminates in a fork with several fine ramifications that enter the synaptic gutters, which are stained for AChR (in red). In the G → A mutant *MuSK* electroporated mouse tibialis anterior muscle, the motor axon stained for 160 kDa neurofilament (in green) exhibits terminal (arrowhead) and ultraterminal sprouts (arrow) running along cup-shaped synaptic gutters (in red). Calibration bar = 20 μm and applies to both prints. (B) Quantitative measurements of nerve terminal length of NMJs of electroporated muscles as illustrated in representative examples in (A). The ratio between the nerve terminal and ultraterminal length over the synaptic gutter length was quantitated in at least 15 NMJs for each condition, i.e. 8 days after electroporation of mouse tibialis anterior muscle with wild-type (WT) *MuSK*, G → A mutant *MuSK*, insC mutant *MuSK* or empty vector (pcDNA3). (C) Quantitative measurements of AChR ε-subunit mRNA in electroporated muscles. pECFP-nuc and wild-type (WT) *MuSK*, G → A mutant *MuSK*, insC mutant *MuSK* or empty vector (pcDNA3) were coelectroporated in tibialis anterior muscles of 5-week-old Swiss Webster male mice. Three days later, the CFP-positive fibers were microdissected. Gene expression was evaluated by quantitative RT-PCR on total RNA extracted from CFP-positive fibers. AChR ε-subunit mRNA levels were normalized to ErbB3. The expression levels of the genes are given as percentages of their expression levels in muscles injected by the empty vector. Error bars correspond to the standard deviation of three independent experiments.

mechanisms were responsible for MuSK dysfunction, we investigated MuSK $-/-$ cells expressing either wild-type MuSK or G \rightarrow A mutated MuSK for their ability to induce AChR aggregation in response to agrin. We found that the G \rightarrow A mutation halved the AChR aggregate number. In addition, agrin-dependent phosphorylation of MuSK was affected by the G \rightarrow A mutation. This change and the fact that the G \rightarrow A mutation is located in the C-terminal part of the protein which contains the catalytic kinase domain prompted us to verify if the G \rightarrow A MuSK mutation was modifying catalytic MuSK activity using an *in vitro* kinase assay after ATP stimulation (12). When comparable amounts of mutated and wild-type MuSK were immunoprecipitated from transfected COS cells, we found that the G \rightarrow A mutation did not affect MuSK catalytic kinase activity. Altogether, these results suggest that the decrease in agrin-dependent AChR aggregation observed with the G \rightarrow A MuSK mutant cannot be attributed to an intrinsic impairment of the catalytic kinase activity but more likely to a lower expression of the mutant MuSK at the muscle membrane.

Effects of the G \rightarrow A mutation on AChR expression and synaptic structure

The analysis of the patient biopsies showed that the G \rightarrow A mutation somehow affects the stimulation of the AChR ϵ -subunit gene and probably of most synaptic genes, because their activation originates from a common mechanism initiated by MuSK (13). The extent of the neurotransmission impairment could be sufficient to result in reduced electrical activity in the muscle fibers, which would activate the myogenic factor myogenin in the extrasynaptic zone and thus ultimately activate the expression of the AChR γ -subunit gene. Altogether, these results suggest that the patient suffers from partial functional dysinnervation.

In mouse skeletal muscle electroporation experiments, where MuSK cDNAs were overexpressed, the G \rightarrow A MuSK was much less efficient in activating the expression of AChR ϵ -subunit mRNA than wild-type MuSK. This could either result from lower levels of G \rightarrow A compared with wild-type MuSK, due to the reduced stability of the mutated protein as observed in C2C12 cells or from a reduction of the intrinsic ability of G \rightarrow A MuSK to activate subsynaptic transcription. It is possible that the G \rightarrow A mutation, by substituting a V for an M in an internal helix of MuSK (24), modifies the spatial conformation of MuSK maybe through a neomorphic mechanism or by altering important interaction sites. This may interfere with the activation of the intracellular cascades controlling postsynaptic differentiation (7,25).

In adult mouse muscle, G \rightarrow A mutant MuSK expression for 8 days was enough to induce dramatic changes in the synaptic structure. These changes were highly reminiscent of those we observed in the patient. In the mouse like in the patient, NMJ were composed of short gutters and small cups. These short NMJs therefore had a reduced surface which could reflect the impairment of the neuromuscular transmission. In both cases also, the axon terminal branches were aberrant: either large terminal boutons covered small AChR clusters, or ultraterminal sprouts failed to find their

target. The presynaptic alterations could simply be a consequence of the functional dysinnervation. Indeed, functional dysinnervation by botulinum toxin (26) or MuSK silencing (23) can cause sprouting. However, in the mouse muscle, the extent of sprouting observed was more prominent than in the patient muscle. In contrast to the axon terminals of the patient which expressed the mature 200 kDa neurofilament (NF-H), mouse axon terminal and sprouts only expressed the immature 160 kDa neurofilament (NF-M) indicating that these nascent axons behaved like embryonic axons (27,28). This suggests that the extent and immaturity of sprouting could be a consequence of the functional denervation and/or the result of an unknown MuSK-dependent retrograde signaling as proposed elsewhere (7,15).

In mouse experiments, the mutated MuSK was expressed in the presence of endogenous MuSK and nevertheless induced the CMS features, which could suggest that the mutated MuSK had a dominant negative effect on wild-type MuSK. This would be in contradiction with the recessive expression of the mutation in human. The most probable explanation is that, owing to the electroporation efficiency, the number of mutated MuSK molecules sufficiently exceeded that of endogenous MuSK to displace it from all its cellular partners and thus, that only the mutated MuSK was functional at the NMJ. Thus, in the mouse model, as in the patient, MuSK function would be entirely performed by the G \rightarrow A mutant. Consistently, the features of the NMJs were very similar in both cases. In other words, the fact that elevated levels of mutated MuSK generated the same effect than in the patient likely shows that the phenotype is not only attributable to reduced levels of MuSK, but rather also to an altered ability of the mutated MuSK to perform its physiological function. Further investigation of the signaling pathway perturbed by the mutation will be highly informative for the identification of the downstream effectors of MuSK.

METHODS

Patient muscle biopsy and mutation analysis

Patient muscle biopsy. A muscle biopsy was taken from deltoid muscles by open biopsy. The neuromuscular junction (NMJ) zone was determined by the small twitch provoked by the tip of the scalpel on the surface of the muscle fascicles. The presence of NMJs was confirmed on a longitudinal strip of the biopsy by revealing cholinesterase activity using the classical Koelle method (29).

Morphological analysis: Whole mounts of specimens fixed with 4% paraformaldehyde were stained for AChR with FITC or TRITC-labeled α -BGT (Molecular Probes, Leiden, The Netherlands), and for neurofilaments with an anti-200 kDa neurofilament antibody (RT 97 clone, Boehringer Ingelheim, Reims, France). The specimens were observed by confocal microscopy (LEICA TCS40, Heidelberg, Germany). Quantitation of the terminal sprouting extent and synaptic gutter length was not possible because of the low number of NMJs in whole mount specimens. In addition, part of the biopsy specimen was processed for immunocytochemical analysis on cryostat sections with TRITC-labeled α -BGT and with a polyclonal antibody raised against MuSK (kindly

donated by Markus Ruegg, Basel, Switzerland). The sections were observed by fluorescence microscopy (Zeiss Axiophot, Oberkochen, Germany). Quantitation of the level of expression of AChR and MuSK was performed by measuring the average fluorescence intensity of bound TRITC- α -BGT to the AChR and bound antibodies to MuSK on CCD-captured images with Metamorph software (Universal Imaging, Westchester, PA, USA).

Quantitative RT-PCR analysis: Total RNA was extracted from 5 to 10 consecutive 10 μ m thick frozen sections of deltoid muscle biopsies using the Qiagen RNeasy mini kit (Qiagen, Courtabœuf, France), with DNase treatments. QRT PCR was performed according to the manufacturer's instructions with the Quantitect one-step RT-PCR SYBRGreen DNA detection kit (Qiagen) in a Light-Cycler (Roche Diagnostics, Meylan, France) Primer sequences were as follows. ϵ -subunit AChR: forward 5'-AGAAATGCACGGTCTC CATC-3', reverse 5'-CGCAATTCATGACAATGAGC-3'; γ -subunit AChR: forward 5'-AACGAGACTCGGATGTG GTC-3', reverse 5'-GTCGCACCAGTCATCTCTA-3'; myogenin: forward 5'-TGGGCGTGAAGGTGTGTA-3', reverse 5'-GGCCTCATTACCTTCTTGA-3'; actin: forward 5'-GGACTCGAGCAAGAGATGG-3', reverse 5'-AGCACT GTGTTGGCGTACAG-3'; ErbB3: forward 5'-GTCTGTGT GACCCACTGCAACT-3', reverse 5'-GGGTGGCAGGAGA AGCATT-3'.

To validate the measures of synapse-specific gene expression, quantification of the expression of the AChR ϵ -subunit and ErbB3 genes, which are never expressed in extra-synaptic regions, were compared to the approximate number of NMJs evaluated by counting cholinesterase-visualized NMJs in the top and bottom sections flanking the sections used for RNA extraction. As expected, the level of AChR ϵ -subunit and ErbB3 expression correlated well with the number of NMJs.

Mutation analysis. DNA from the affected patient and living family members was extracted from peripheral blood lymphoblastoid cells by standard protocols. For the deceased child, DNA was obtained by scraping a muscle biopsy section made and mounted in Canada balsam 24 years ago. Fifteen sets of primers were designed according the published sequence of *MUSK* (GenBank accession number AF006464) in order to amplify each of the 14 exon intronic flanking regions. They can be provided on demand. PCR was carried out with: DNA 100 ng, dNTP 1 μ M, each primer 0.5 μ M, Enhancer (Tebu, Le Perray en Yvelines, France) 1 \times MgCl₂ 1.5 mM, and Ampli Taq Gold 1 unit (Applied Biosystems, Courtabœuf, France). All fragments were amplified in a unique condition consisting of a touch down protocol including a hybridization step at 65 to 55°C (10 cycles, 1°C per cycle) followed by 25 cycles at 55°C. PCR fragments were then sequenced using the Big Dye Terminator (V3.1) Cycle Sequencing Kit (Applied Biosystems) and sequencing reactions were loaded on an ABI PRISM 3100 Genetic analyzer and analyzed with Seqscape software. Any variant was confirmed as a disease-causing mutation by analysis of cosegregation in affected members of family, conservation of the residue among species and isoforms and absence in 200 control chromosomes of healthy adults.

Experimental expression of mutated MuSK

Site-directed mutagenesis. In the intracellular domain, sequences between rat and human are highly homologous (16). This allowed us to use a pcDNA 3 vector containing rat *MuSK* cDNA kindly given by Dr Werner Hoch (University of Houston, Houston, USA) Mutagenesis was performed by the method of Kunkel *et al.* (30) and allowed us to obtain constructs bearing the same mutations of *MUSK* as found in the patient.

Expression study in COS cells. The expression vectors for wild-type or mutated *MuSK* were co-transfected in COS-7 cells with pEGFP-N1 vector (Clontech, Ozyme, St Quentin en Yvelines, France) using Exgen 500 reagent (Euromedex, Souffelweyersheim, France) according to the manufacturer's recommendations. COS-7 cells were cultured with Dulbecco's modified Eagle's medium (DMEM, Invitrogen) supplemented with 10% fetal calf serum. Cells were maintained in a 5% CO₂ incubator at 37°C. Twenty-four hours after transfection, the transfected COS-7 cells were washed with phosphate-buffered saline and were homogenized in lysis buffer (10 mM Tris-HCl pH 7.4, 5 mM EDTA, 150 mM NaCl, 10 μ g/ml leupeptin, 25 μ g/ml aprotinin, 10 μ g/ml pepstatin and 2% Triton X-100). After centrifugation (8 min at 10 000 rpm), the solubilized proteins were collected and the amount was estimated using the BCA kit (Pierce, Rockford, USA).

Samples were boiled for 3 min and separated on 10% SDS-PAGE under reducing conditions and then transferred to nitrocellulose membranes (Novex). The blots were blocked in 10% milk in PBS. The membranes were incubated with the C-terminal anti-MuSK polyclonal antibody (21) or with anti-MuSK N-term antibody (catalog AP7664a, Abgent, San Diego, CA, USA) at 4°C overnight (22). They were also probed with a GFP monoclonal antibody (Clontech, Ozyme) to check transfection efficiencies. After labeling, membranes were washed and then incubated with horseradish peroxidase-conjugated anti-rabbit or anti-mouse secondary antibodies (Dako, Carpinteria, CA, USA). Membranes were developed by enhanced chemiluminescence using the ECL kit (Pierce). Densitometry analysis of bands was done using Scion image software.

Functional studies using MuSK -/- muscle cells. Retroviral infection of MuSK -/- muscle cells: Retroviral infections of myoblasts were performed as described previously (12). Briefly, Bosc 23 cells were transfected with pBabe/puro-MuSK wild-type and pBabe/puro-G/AMuSK, and virus-containing medium was collected 2 days post-transfection and used immediately for infection. Myoblasts, at 50% confluency, were incubated with virus-containing medium, supplemented with 2 μ g/ml polybrene (Sigma), for 2 h at 33°C. Infected myoblasts were selected in growth medium containing puromycin (2 μ g/ml) and clones of cells were isolated. Clonal cells were subsequently cultured as myoblasts at 33°C/10% CO₂ on dishes precoated with Matrigel (Becton Dickinson France, Le Pont de Claix, France) in growth medium [DMEM containing 10% heat-inactivated fetal bovine serum (FBS), 10% horse serum (HS), 1% glutamine, penicillin, streptomycin, gentamicin] supplemented with

20 U/ml of recombinant mouse interferon- γ (IFN- γ ; Life Technologies, Cergy-Pontoise, France). To induce myotube formation, cultures were transferred to 39°C/10% CO₂ and the medium was replaced with DMEM containing 10% HS, 1% glutamine, and antibiotics, but no FBS or IFN- γ .

AChR clustering assay: Myotubes stably expressing MuSK were stimulated with a recombinant rat C-terminal fragment of agrin (50 ng/ml, R&D Systems Inc., Minneapolis, MN, USA) for 24 h. Myotubes were washed with PBS, fixed for 10 min at room temperature in 4% paraformaldehyde in PBS and then washed three times with 0.1 M glycine in PBS. Then they were incubated for 1 h with TRITC- α -BGT (Molecular Probes). AChR clustering was quantified by counting the number of AChR clusters >3 μ m in length using a 20 \times objective in 15 fields of each Petri dish. This number was divided by the number of labeled myotubes that crossed the field. The culture dishes were observed under a reversed Olympus IX70 fluorescence microscope (Olympus Europa, Hamburg, Germany) using appropriate filters. Images were recorded with a CCD camera (Princeton Cool SNAP Fx, Trenton, NJ) and processed with Metamorph software. Three independent experiments were performed with three G \rightarrow A mutant *MuSK* clones expressing levels of MuSK comparable to the levels of MuSK from wild-type MuSK cell line as checked by western blot. Myotubes were extracted in 1% Nonidet P40 in lysis buffer (21) and immunoblot was performed as described earlier for COS cells. Alpha-tubulin monoclonal antibody (DM1A, Sigma) was used to check protein load.

MuSK tyrosine phosphorylation: Myotubes stably expressing MuSK were simulated by agrin as described earlier and extracted in 1% Nodinet-P40 in lysis buffer (21). Cleared lysates were incubated with MuSK polyclonal antibody to precipitate MuSK. Bead-precipitated proteins were eluted into SDS sample buffer, subjected to SDS-PAGE and analyzed by phosphotyrosine immunoblotting (mAb 4G10, Upstate Biotechnology, Lake Placid, NY, USA). Blots were stripped and reprobed with MuSK polyclonal antibody (21).

Stability of mutant *MuSK* in C2C12 cells. Expression constructs and cell transfection: Full-length cDNAs encoding HA-tagged wild-type and G \rightarrow A mutant MuSK were sub-cloned into the *KpnI*-*XbaI* sites of the pCDNA3 vector (Invitrogen). The cDNAs encoding HA-tagged wild-type and mutant MuSK were obtained by PCR with the T7 oligonucleotide primer and 5'GATCTCTAGAGAATTCTCAAGCGTAGTCTGGGACGTCGTATGGGT ATGCGACGCCTACCGTTCCCTCTGCTC 3' (antisense primer containing the last 23 bp of MuSK cDNA excluding the stop codon followed by the HA-tag sequence, a stop codon and an *XbaI* site). Cell transfections were performed with Fugene (Roche Molecular Biochemicals) reagent according to the manufacturer's instructions.

Cycloheximide treatment: C2C12 cells were transfected with pcDNA3-HA-tagged wild-type and mutant MuSK. Following 36 h of transfection, cells were treated with cycloheximide (Sigma) at 15 μ g/ml for the indicated times and lysates were prepared for analysis. Cotransfection of a plasmid expressing GFP allowed estimation of transfection efficiency.

Wild-type and mutant HA-MuSK were detected by western blot analysis with a polyclonal anti-HA antibody (12CA5, Roche Molecular Biochemicals). Alpha-tubulin was used as an internal control and detected with a monoclonal antibody (DM1A, Sigma). GFP was detected with an anti-GFP antibody (sc-9996, Santa Cruz Biotechnology).

In vitro kinase assays in COS cells. COS cells were transfected with pcDNA3-HA-tagged wild-type and mutant MuSK. Cotransfection of a plasmid expressing GFP with the MuSK expression plasmids allowed the estimation of the transfection efficiency to 51–52% by FACS quantification of GFP-positive cells. Following 36 h of transfection, cells were lysed in 1% NP40, 20 mM HEPES pH 7.4, 150 mM NaCl, 1 mM EDTA, 1 mM EGTA, protease inhibitors (Complete, Roche Molecular Biochemicals). Protein concentrations in lysates were determined with a DC kit (Biorad) and similar amounts of total protein were subjected to immunoprecipitation with a monoclonal anti-HA antibody (clone HA-11, Babco). Beads were washed three times with lysis buffer and one time with kinase buffer (20 mM HEPES pH 7.4, 10 mM MnCl₂ and 0.1 mM vanadate). The beads were then incubated in 40 μ l of kinase buffer containing 5 μ Ci of (γ -³²P) ATP (3000 Ci/mmol, Amersham), 0.1 mM vanadate for 30 min at 30°C. Proteins were then resolved by SDS-PAGE, and radio-labeled proteins were detected by phosphoimager analysis. For exogenous substrate phosphorylation, 50 μ g of a poly-glutamate/lysine/tyrosine peptide, p(EKY) (Sigma) was added to the kinase reaction and incubated for 30 min at 30°C. The reactions were stopped by adding 40 μ l of ice-cold trichloroacetic acid (TCA) and mixtures were then centrifuged for 2 min. Supernatants were collected and incubated for 10 min on ice with 1 ml of ice-cold 10% TCA, 100 μ g BSA, 100 mM sodium pyrophosphate. Precipitates were harvested on glass fiber filters and counted in a β -counter.

In vivo expression in mouse tibialis anterior muscle. All animal studies were approved by animal use procedures adopted by INSERM.

Plasmids and electroporation: Swiss Webster mice, 5–10-week-old, were anesthetized with 300 μ l of 0.05% xylazine–1.7% ketamine in 0.9% NaCl. 7 μ g of DNA containing 5 μ g of the wild-type or mutated MuSK expression vectors and 2 μ g of reporter plasmid were injected into the tibialis anterior muscle using a 1 ml syringe with a 27 gauge needle. Caliper electrode plates (Qbiogen, Illkirch, France) were then applied to each side of the muscle, and a series of eight electrical pulses (2 Hz, 20 ms each) was delivered with a standard square-wave electroporator (ECM 830, Qbiogen) (31). Electrical contact was ensured by shaving and conductive gel application. The reporter construct allowed the identification of electroporated fibers, and consisted of expression vectors for a nuclear CFP (pECFPnuc, Clontech, Ozyme) (32).

Morphological analysis: Morphological analysis of the end-plate was performed by confocal microscopy as described above for the patient muscle biopsy. We used both a 160 and a 200 kDa neurofilament antibody. For quantitative measurements we used only sections immunostained with a 160 kDa neurofilament antibody. To quantitate the extent of terminal sprouting, we measured the ratio between the

synaptic gutter length and the amyelinic nerve terminal and ultraterminal length of at least 15 NMJs in each experimental condition using LUCIA image analysis software.

Quantitative RT-PCR: Total RNA was extracted from dissected muscle fibers and gene expression was analyzed by QRT-PCR as for human biopsies. AChR α : forward 5'-CTTGGTGCTGCTCGCTTACTT-3', reverse 5'-CGTTGATAGAGACCGTGCATTTTC-3'; β -actin: forward 5'-CCCTGTATGCCTCTGGTCGT-3', reverse 5'-ATGGCGTGAGGGA GAGCAT-3'; ErbB3: forward 5'-CTTACGGGACACAAT GCTGA-3', reverse 5'-GCATGGCTGGAGTTGGTATT-3'.

ACKNOWLEDGEMENTS

We are grateful to Markus Ruegg and Christian Fuhrer for their gift of anti-MuSK antibodies, to Werner Hoch for his gift of rat *MuSK* cDNA vector, to Steve Burden for providing his MuSK $-/-$ muscle cells and to Hans Peter Seelig for MuSK autoantibody testing. We thank Andrée Rouche for her help in quantitative morphological analysis. We express gratitude to Eric Krejci, Marion Paturneau-Jouas and Veit Witzemann for critical reading of this manuscript. This work was supported by INSERM, Assistance Publique-Hôpitaux de Paris (PHRC AOM 1036), AFM, and GIS-Institut des Maladies Rares.

REFERENCES

- Engel, A.G., Ohno, K. and Sine, S.M. (2003) Congenital myasthenic syndromes: progress over the past decade. *Muscle Nerve*, **27**, 4–25.
- Hantaï, D., Richard, P., Koenig, J. and Eymard, B. (2004) Congenital myasthenic syndromes. *Curr. Opin. Neurol.*, **17**, 539–551.
- Ohno, K., Engel, A.G., Shen, X.M., Selcen, D., Brengman, J., Harper, C.M., Tsujino, A. and Milone, M. (2002) Rapsyn mutations in humans cause neuromuscular junction acetylcholine-receptor deficiency and myasthenic syndrome. *Am. J. Hum. Genet.*, **70**, 875–885.
- Richard, P., Gaudon, K., Andreux, F., Yasaki, E., Prioleau, C., Bauché, S., Barois, A., Ioos, C., Mayer, M., Routon, M.C. *et al.* (2003) Possible founder effect of rapsyn-N88K mutation and identification of novel rapsyn mutations in congenital myasthenic syndromes. *J. Med. Genet.*, **40**, e81.
- Gautam, M., Noakes, P.G., Mudd, J., Nichol, M., Chu, G.C., Sanes, J.R. and Merlie, J.P. (1995) Failure of postsynaptic specialization to develop at neuromuscular junctions of rapsyn-deficient mice. *Nature*, **377**, 232–236.
- Gautam, M., Noakes, P.G., Moscoso, L., Rupp, F., Scheller, R.H., Merlie, J.P. and Sanes, J.R. (1996) Defective neuromuscular synaptogenesis in agrin-deficient mutant mice. *Cell*, **85**, 525–535.
- DeChiara, T.M., Bowen, D.C., Valenzuela, D.M., Simmons, M.V., Poueymirou, W.T., Thomas, S., Kinetz, E., Compton, D.L., Rojas, E., Park, J.S. *et al.* (1996) The receptor tyrosine kinase MuSK is required for neuromuscular junction formation *in vivo*. *Cell*, **85**, 501–512.
- Glass, D.J., Bowen, D.C., Stitt, T.N., Radziejewski, C., Bruno, J., Ryan, T.E., Gies, D.R., Shah, S., Mattsson, K., Burden, S.J. *et al.* (1996) Agrin acts via a MuSK receptor complex. *Cell*, **85**, 513–523.
- Sanes, J.R. and Lichtman, J.W. (2001) Induction, assembly, maturation and maintenance of a postsynaptic apparatus. *Nat. Rev. Neurosci.*, **2**, 791–805.
- Sander, A., Hesser, B.A. and Witzemann, V. (2001) MuSK induces *in vivo* acetylcholine receptor clusters in a ligand-independent manner. *J. Cell Biol.*, **155**, 1287–1296.
- Bezakova, G. and Ruegg, M.A. (2003) New insights into the roles of agrin. *Nat. Rev. Mol. Cell. Biol.*, **4**, 295–308.
- Herbst, R. and Burden, S.J. (2000) The juxtamembrane region of MuSK has a critical role in agrin-mediated signaling. *EMBO J.*, **19**, 67–77.
- Schaeffer, L., de Kerchove d'Exaerde, A. and Changeux, J.P. (2001) Targeting transcription to the neuromuscular synapse. *Neuron*, **31**, 15–22.
- Woldeyesus, M.T., Britsch, S., Riethmacher, D., Xu, L., Sonnenberg-Riethmacher, E., Abou-Rebyeh, F., Harvey, R., Caroni, P. and Birchmeier, C. (1999) Peripheral nervous system defects in *erbB2* mutants following genetic rescue of heart development. *Genes Dev.*, **13**, 2538–2548.
- Nguyen, Q.T., Son, Y.J., Sanes, J.R. and Lichtman, J.W. (2000) Nerve terminals form but fail to mature when post-synaptic differentiation is blocked: *in vivo* analysis using mammalian nerve-muscle chimeras. *J. Neurosci.*, **20**, 6077–6086.
- Valenzuela, D.M., Stitt, T.N., DiStefano, P.S., Rojas, E., Mattsson, K., Compton, D.L., Nunez, L., Park, J.S., Stark, J.L., Gies, D.R. *et al.* (1995) Receptor tyrosine kinase specific for the skeletal muscle lineage: expression in embryonic muscle, at the neuromuscular junction, and after injury. *Neuron*, **15**, 573–584.
- Selcen, D., Fukuda, T., Shen, X.-M. and Engel, A.G. (2004) Are MuSK antibodies the primary cause of myasthenic symptoms? *Neurology*, **62**, 1945–1950.
- Ip, F.C.F., Glass, D.G., Gies, D.R., Cheung, J., Lai, K.O., Fu, A.K.Y., Yancopoulos, G.D., and Ip, N.Y. (2000) Cloning and characterization of muscle-specific kinase in chicken. *Mol. Cell. Neurosci.*, **16**, 661–673.
- Trinidad, J.C., Fischbach, G.D., and Cohen, J.B. (2000) The Agrin/MuSK signaling pathway is spatially segregated from the neuregulin/ErbB receptor signaling pathway at the neuromuscular junction. *J. Neurosci.*, **20**, 8762–8770.
- Tang, J., Jo, A.J., and Burden, S.J. (1994) Separate pathways for synapse-specific and electrical activity-dependent gene expression in skeletal muscle. *Development*, **120**, 1799–1804.
- Fuhrer, C., Sugiyama, J.E., Taylor, R.G. and Hall, Z.W. (1997) Association of muscle-specific kinase MuSK with the acetylcholine receptor in mammalian muscle. *EMBO J.*, **16**, 4951–4960.
- Zhou, H., Glass, D.J., Yancopoulos, G.D. and Sanes, J.R. (1999) Distinct domains of MuSK mediate its abilities to induce and to associate with postsynaptic specializations. *J. Cell Biol.*, **146**, 1133–1146.
- Kong, X.C., Barzaghi, P. and Ruegg, M.A. (2004) Inhibition of synapse assembly in mammalian muscle *in vivo* by RNA interference. *EMBO Rep.*, **5**, 1983–1988.
- Till, J.H., Becerra, M., Watty, A., Lu, Y., Ma, Y., Neubert, T.A., Burden, S.J. and Hubbard, S.R. (2002) Crystal structure of the MuSK tyrosine kinase: insights into receptor autoregulation. *Structure*, **10**, 1187–1196.
- Burden, S.J. (2002) Building the vertebrate neuromuscular synapse. *J. Neurobiol.*, **53**, 501–511.
- Tian, W.-H., Festoff, B.W., Blot, S., Diaz, J. and Hantaï, D. (1995) Synaptic transmission blockade increases plasminogen activator activity in mouse skeletal muscle poisoned with botulinum toxin type A. *Synapse*, **20**, 24–32.
- Carden, M.J., Trojanowski, J.Q., Schlaepfer, W.W. and Lee, V.M.-Y. (1987) Two-stage expression of neurofilament polypeptides during rat neurogenesis with early establishment of adult phosphorylation patterns. *J. Neurosci.*, **7**, 3489–3504.
- Julien, J.P. (1999) Neurofilament functions in health and disease. *Curr. Opin. Neurobiol.*, **9**, 554–560.
- Koelle, G.B. and Friedenwald, J.S. (1949) A histological method for localization of cholinesterase activity. *Proc. Soc. Exp. Biol. Med.*, **70**, 617–622.
- Kunkel, T.A., Roberts, J.D. and Zakour, R.A. (1987) Rapid and efficient site-specific mutagenesis without phenotypic selection. *Methods Enzymol.*, **154**, 367–382.
- Mir, L.M., Bureau, M.F., Gehl, J., Rangara, R., Rouy, D., Caillaud, J.-M., Delaere, P., Branell, D., Schwartz, B. and Scherman, D. (1999) High-efficiency gene transfer into skeletal muscle mediated by electric pulses. *Proc. Natl Acad. Sci. USA*, **96**, 4262–4267.
- Duclert, A., Savatier, N. and Changeux, J.P. (1993) A 83-nucleotide promoter of the acetylcholine receptor epsilon-subunit gene confers preferential synaptic expression in mouse muscle. *Proc. Natl Acad. Sci. USA*, **90**, 3043–3047.